

Article

Effects of Wheat and Rapeseed Production on Soil Water Storage in Mongolian Rangeland

Katori Miyasaka ^{1,*}, Takafumi Miyasaka ², Jumpei Ota ¹, Siilegmaa Batsukh ³ and Undarmaa Jamsran ⁴

¹ College of Bioresource Sciences, Nihon University, 1866 Kameino, Fujisawa-shi 252-0880, Kanagawa, Japan; hayabusa_jun0826@yahoo.co.jp

² Graduate School of Environmental Studies, Nagoya University, Furo-cho, Chikusa-ku, Nagoya-shi 464-8601, Aichi, Japan; miyataka@nagoya-u.jp

³ School of Geology and Mining Engineering, Mongolian University of Science and Technology, P.O. Box 46/338, Ulaanbaatar 210646, Mongolia; siileg_hydro@must.edu.mn

⁴ Center for Ecosystem Studies, Mongolian University of Life Sciences, Ulaanbaatar 17024, Mongolia; j_undarmaa@mul.edu.mn

* Correspondence: miyasaka.katori@nihon-u.ac.jp; Tel.: +81-466-84-3696

Abstract: In recent years, Mongolia has witnessed an increase in not only wheat fields, which have been present for a long time, but also rapeseed fields. This has led to increasing concerns about soil degradation due to inappropriate cultivation. This study aims to determine the impacts of rapeseed production on soil water storage in Mongolia. The soil water content and matric potential were measured in wheat and rapeseed fields and adjacent steppe rangeland for five years, including crop production and fallow years, and the soil water storages in the fields were compared. The results demonstrated that the matric potential below the root zone in the rapeseed field and both rangelands was drier than the wilting point, whereas the potential in the wheat field was usually almost the same or wetter than this point. The comparison of the amount of soil water storage during the fallow year with that of the adjacent rangeland showed it to be 5–10% higher for the wheat field and almost equal for the rapeseed field. Field management must consider the fact that rapeseed fields use more water than is required by wheat fields and that less water is stored during fallow periods.

Keywords: canola; crop management; soil water content; matric potential



check for updates

Citation: Miyasaka, K.; Miyasaka, T.; Ota, J.; Batsukh, S.; Jamsran, U. Effects of Wheat and Rapeseed Production on Soil Water Storage in Mongolian Rangeland. *Agriculture* **2021**, *11*, 888. <https://doi.org/10.3390/agriculture11090888>

Academic Editor: Aliasghar Montazar

Received: 28 July 2021

Accepted: 5 September 2021

Published: 15 September 2021

Publisher's Note: MDPI stays neutral with regard to jurisdictional claims in published maps and institutional affiliations.



Copyright: © 2021 by the authors. Licensee MDPI, Basel, Switzerland. This article is an open access article distributed under the terms and conditions of the Creative Commons Attribution (CC BY) license (<https://creativecommons.org/licenses/by/4.0/>).

1. Introduction

The Mongolian steppe, located in cold and dry areas, is unfit for crop farming because of the short growing season for plants and the low amounts of precipitation. Therefore, nomadic livestock farming, i.e., moving from place to place with livestock such as camels, horses, cattle, *sheep*, and goats, in search of water and grass, has been the main agricultural approach since ancient times. However, with the introduction of the Virgin Lands campaign of the Soviet Union in 1959, Mongolia intensified its efforts to expand crop production. The main crops that were cultivated were cereals (of which, wheat comprised ~80%), potatoes, fodder crops, and some vegetables [1] (Figure 1). The area of cultivated land increased sharply until around 1990. However, with the collapse of the Soviet Union at the end of 1991, Mongolia transitioned from a socialist economic system to a free market economic system in 1992. Farms were decentralized and became privately owned. Consequently, the increased cost of operation for individual farmers led to a sharp reduction in the cropland area and an increase in cropland abandonment (Figure 1). In 2008, triggered by the “Third Virgin Land Program (Atar-III)”, the Mongolian government promoted the reuse of abandoned lands as croplands to improve food self-sufficiency [2]. Consequently, the plantation area has begun to increase again (Figure 1). Moreover, in the 2000s, rapeseed (*Brassica napus* L.) began to be considered as a major alternative to wheat for large-scale production due to limited export opportunities of wheat in contrast to the almost limitless

Chinese demand for oil and energy crops [3]. Therefore, the rapeseed field area has been increasing since the mid-2000s (Figure 1).

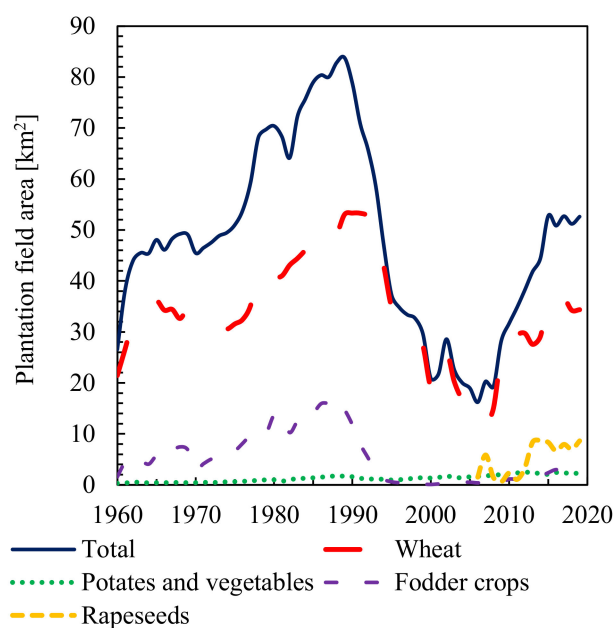


Figure 1. Changes in the field area of Mongolia from 1960 to 2019 [1].

However, rapeseed is characterized by high water and nitrogen requirements [4–7], deeper roots [8], and susceptibility to disease and insects [9]. In field areas where rainfed agriculture is practiced in arid regions, such as Mongolia, water is an especially limiting factor in crop production, and there is a strong correlation between yield and precipitation [10]. Therefore, the high-water requirement of rapeseed may have a significant impact on the soil water storage of a field.

Orgil [11] interviewed Mongolian farmers on the impact of rapeseed production on the environment and found that 52% of the interviewees felt that rapeseed production would have a negative impact on the environment and 22% felt that it would have no impact, while only 6.0% felt that it would have a beneficial impact. The farmers cited the lack of a comprehensive policy on environmental protection in the agricultural sector and the lack of research on the effects of rapeseed production on soil as factors contributing to the negative impact [11].

Currently, most Mongolian farmers use outdated machinery and apply the same planting and harvesting methods for rapeseed production as those used for wheat [11]. The risk introduced by poor farm management can deteriorate the quality and yield of farm products [12], resulting in the abandonment of these croplands. Cropland abandonment is expected to result in land degradation including soil erosion, reduced species richness, and a decrease in the cover of perennial grasses [13–17].

Therefore, it is necessary to clarify the impact of rapeseed production on soil environment and provide suitable management methods for rapeseed production. However, few studies have investigated the negative effect of rapeseed production on soil environment.

Among the effects of rapeseed production on soil environment, this study focuses on soil water storage and aims to clarify the effects of rapeseed production, which has been increasing in recent years, on soil water content and matric potential, and demonstrate how rapeseed production differs from the production of wheat, which has been produced in Mongolia over a long time. We analyzed soil water storage in wheat fields, rapeseed fields, and adjacent grassland areas for five years, including crop production and fallow years.

2. Materials and Methods

2.1. Study Area

The study area was in the western part of Argalant *soum* (district), Töv province, Mongolia (47°48' N, 105°53' E), which is one of the main regions for wheat and rapeseed production [3] (Figure 2). Data from a weather station at Hustai National Park, located 11–13 km southeast of the selected study area (47°42' N, 105°56' E), indicated that the average annual temperature and annual precipitation were 0.2 °C and 213 mm during 2005–2017 (Figure 3). The area received 90% of its annual rainfall during the period of May–September.

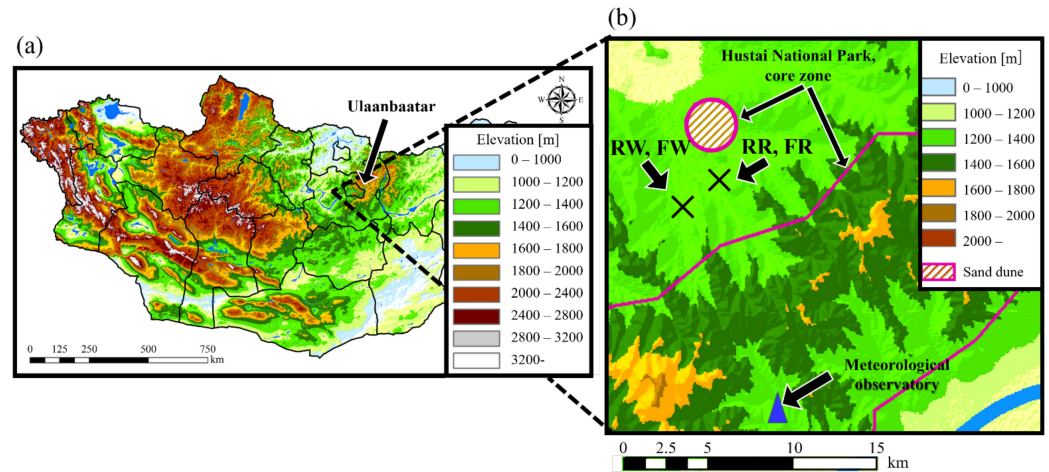


Figure 2. Map of study area. (a) Study area located near Hustai National Park, Mongolia and (b) Survey sites. FR: rapeseed field; FW: wheat field; RR: rangeland adjacent to FR; RW: rangeland adjacent to FW.

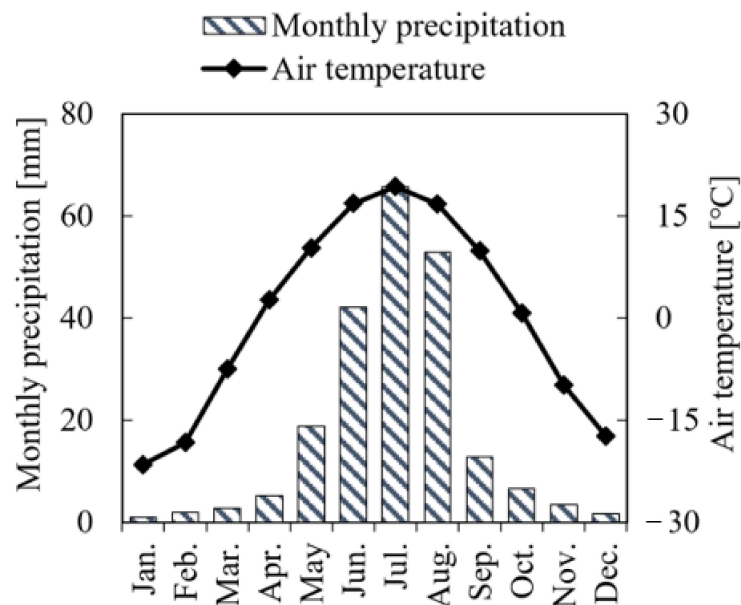


Figure 3. Monthly average precipitation and air temperature obtained from a weather station at Hustai National Park located 11–13 km southeast of the study sites during the period of 2005–2017.

Under the socialist system, a national farming company used to produce wheat in Argalant *soum*; however, a considerable area of the cropland was abandoned around the year 2000. The abandoned cropland has since been recultivated under the recent agricultural policy. Although wheat remains a major crop species in this area, the production of rapeseed has seen a gradual increase. In this area, the groundwater level is low, rain-

fed agriculture is practiced, and water is the limiting factor in crop production. Water is obtained from snowmelt and precipitation [3], and a two-field system has been adopted. In this system, one field is used for sowing crops, while another field of an equal size is left fallow, and the use of these two fields is switched in the subsequent year. This system maintains soil fertility, prevents replanting failures, and ensures weed control; however, its largest merit is increased soil water storage.

In general, the annual evapotranspiration of rangeland in arid lands is almost equal to the annual precipitation [18,19], with a few exceptions such as areas with shallow groundwater tables. In cultivated land, the evapotranspiration by crops is also basically equal to the annual precipitation, although the depth of water absorption may be greater than that of rangeland plants [20]. However, by keeping some land fallow, some of the precipitation stored during the fallow period is carried over to the next year, so the annual evapotranspiration in the cultivated land exceeds the annual precipitation [21–23], and the yield will increase compared to the case where no land is kept fallow. The amount of water stored during fallow periods varies greatly depending on the soil type, weather conditions, and how the farmland is managed [21]. Therefore, we interviewed local cropland managers and experts and selected two typical cultivated fields as the sampling sites. We selected these particular fields because we had sufficient information about their management and history, and because the climatic conditions and soil type are almost the same. The selected wheat field (FW) was managed by a national farming company from 1978 to 1990 and subsequently by privatized company until 1999 (Figure 4a).

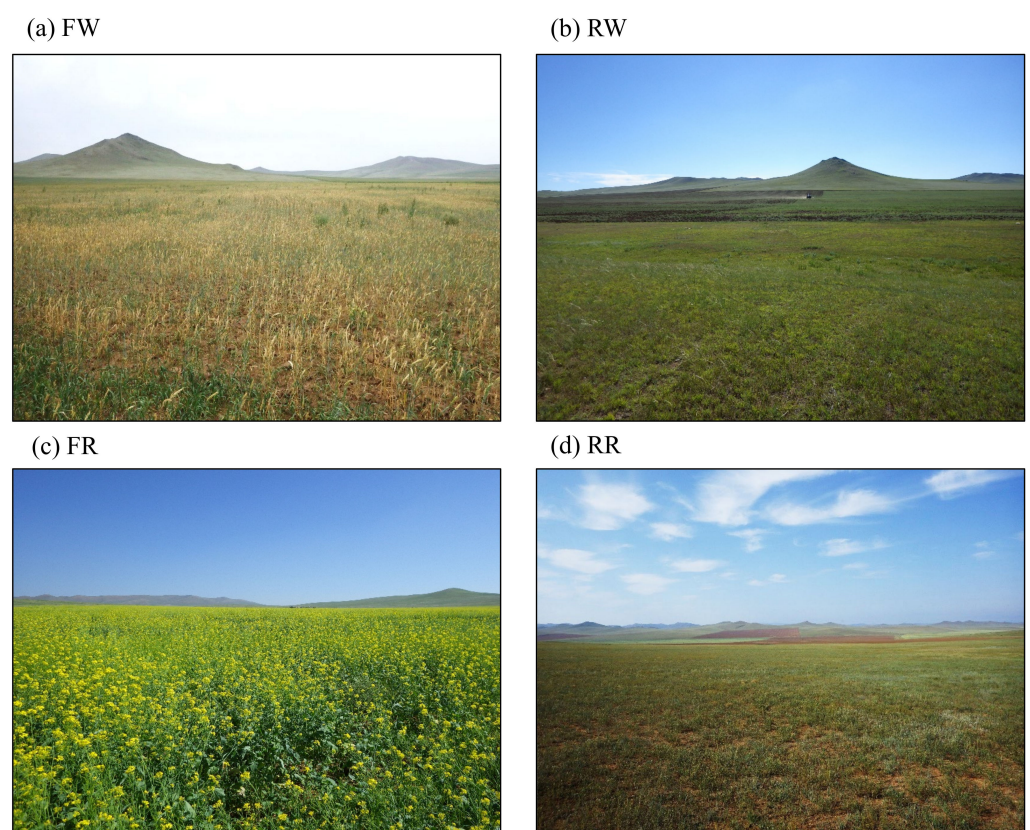


Figure 4. Photographs of the study sites taken in the summer of 2015. (a) Wheat field in a production year (FW), (b) rangeland adjacent to the wheat field (RW), (c) rapeseed field in a production year (FR), and (d) rangeland adjacent to the rapeseed field (RR).

Although this cropland was abandoned from 2000 to 2004, another private company recultivated the land in 2005. The land has been used to grow wheat since then. In a production year, seeds are sown from early to late May, and crops are harvested from September to October. In a fallow year, the field is plowed twice a year to a depth of 20 cm.

As compound fertilizers containing K, N, and P are expensive for farmers, only some of the purchased fertilizer was applied to the fields.

The selected rapeseed field (FR) had a similar history to that of FW: the same national and privatized companies produced wheat in this field for the same time periods and abandoned it from 2000 to 2008; the private company managing FW recultivated this abandoned field in 2009 (Figure 4c). Wheat was produced in this field until 2013; however, rapeseed began to be grown instead of wheat in 2014. In a production year, the sowing period of rapeseed is from late May to early June, which is later than that of wheat, and crops are harvested after reaping wheat, from September to late October. In a fallow year, the field is plowed twice a year to a depth of 20 cm, the same as FW. FR has not been fertilized since it began to be used for cultivation in 2009.

The two field sites were ~3 km apart. We investigated the rangeland adjacent to FW (RW) and FR (RR) as controls (Figure 4b,d). The rangeland sites were sufficiently flat to prevent surface runoff. The study area is classified as a winter camping area, which allows livestock, such as cattle, horses, sheep, and goats, to enter the cropland from around October after the end of the harvest to the April of the following year, when sowing begins.

Table 1 describes the information for all study sites. All the study sites have *Kastanozems* as the soil type and the same light clay soil texture.

Table 1. Characteristics of the four study sites in Mongolia.

Site	RR	FR	RW	FW
Location				
N	47° 48' 39.9"	47° 48' 39.0"	47° 47' 16.1"	47° 47' 15.8"
E	105° 53' 26.5"	105° 53' 26.3"	105° 52' 6.1"	105° 52' 2.8"
Land use	Rapeseed production	Rangeland	Wheatproduction	Rangeland
Soil type	<i>Kastanozems</i> [24] (Chestnut soil)	<i>Kastanozems</i> [24] (Chestnut soil)	<i>Kastanozems</i> [24] (Chestnut soil)	<i>Kastanozems</i> [24] (Chestnut soil)
Texture ^a	Light clay	Light clay	Light clay	Light clay
Coarse sand	4.5%	9.0%	7.8%	4.8%
Fine sand	29.2%	38.0%	41.8%	32.2%
Silt	31.5%	24.6%	21.4%	28.4%
Clay	34.8%	28.4%	29.0%	34.6%

^a For all sites, the particle size of the soil was measured from 0 to 5 cm in accordance with ISO 17892-4; 2016, which is measured by sieving or sedimentation according to particle size. The soil texture classes were defined according to the International Society of Soil Science Soil classification system: clay (<0.002 mm), silt 0.002–0.02 mm), fine sand (0.02–0.2 mm), and coarse sand (0.2–2 mm).

2.2. Soil Sampling Method and Period

The soil sampling surveys were conducted at 10 cm intervals and depths of 0–100 cm mainly using a soil auger (inner diameter: approximately 3 cm) and rarely using a soil rod (inner diameter: approximately 1 cm) to measure the vertical profiles of the soil water content during the following eight periods at all study sites: 26–28 October 2015; 9–10 August and 2–3 November 2016; 29 April–2 May and 28–30 October 2017; 19 June and 17 November 2018; and 16 August 2019. The dry soil weight per 10 cm depth was more than 30 g when the soil auger was used and approximately 10 g when the soil rod was employed. A few replicate samples were obtained at all sites during each period. The fallow periods of FW were 2016 and 2018 and those of FR were 2016, 2018, and 2019 (Table 2). The soil samples in October 2015 and 2017 were obtained after harvesting and that in August 2019 in FW was obtained during the peak wheat growing season.

Table 2. Production history and annual precipitation from 2014 to 2019 in FR and FW. The annual precipitation was obtained from a weather station at Hustai National Park located 11–13 km southeast of the study sites.

Site	2014	2015	2016	2017	2018	2019
Annual precipitation (mm)	224	176	192	182	217	193
FR	P	P	F	P	F	F
FW	P	P	F	P	F	P

P: production year, F: fallow year.

2.3. Method of Measuring Soil Water Content, Matric Potential, and Bulk Density

The soil at 10 cm intervals and depths of 0–100 cm was dried by conductive heating through the direct application of heat (temperature greater than 110 °C) to the specimen container using a gas stove for approximately 1 h (See Appendix A and Table A1). The weights of the wet soils before heating and the dry soils after heating were measured using a scale (minimum reading: 0.01 g), and the soil water contents were calculated gravimetrically using the following equation:

$$w_c = \frac{M_w - M_d}{M_d}, \quad (1)$$

where w_c is the gravimetric soil water content (g/g), M_w is the mass of moist soil (g), and M_d is the mass of the dried soil (g).

The soil water potentials were measured directly by taking about 10 g off the soil samples collected using the auger method and measuring the soil with a soil psychrometer (SC10A, Decagon Devices, Logan, UT, USA) in August 2016, April 2017, and June 2018. In these areas, the soil water salinity is very low and the contribution of osmotic potential to the water potential is sufficiently small; therefore, the water potential can be considered to be equal to the matric potential. The soil water characteristic curves at all sites were estimated according to the relationship between the matric potential and soil water content. The matric potentials that were not measured directly were calculated using the soil water characteristic curves.

The bulk densities 10 cm intervals were measured using either a 100 cm³ soil sampler (inner diameter: 5 cm, height: 5.1 cm) at depths of 0–15 cm and the auger (inner diameter: approximately 3 cm, cross-sectional area: 8.75 cm²) at depths of 15–60 cm in October 2015 and August 2016. The auger has almost completely semi-cylindrical, cut edges that are equidistant running from the top to the bottom.

The 100 cm³ sampler was hammered every 5 cm from the surface layer to a depth of 15 cm, the soil that protruded from the top and bottom of the sampler was carefully scraped off with a knife, and the soil core was sampled in a cylindrical shape with a diameter of 5 cm and a length of 5.1 cm. The soil was dried using the method described earlier, and its dry density was calculated by dividing the dry soil weight by the sampler volume.

For the auger, soil samples were collected from the surface layer to a depth of 60 cm by hammering the auger every 30 cm, rotating it and pulling it out to collect cylindrical soil samples. Soil protruding from the auger was carefully scraped off and formed into a 30-cm-long, semi-circular cylinder. The length was cut into 10 cm pieces and the dry density was calculated using the same method as in the case of the 100 cm³ sampler.

The volumetric water content measured during the two surveys was averaged for each depth and was calculated by multiplying the soil water content with the dry density.

2.4. Estimation of Soil Water Characteristic Curves

For the soil samples whose matric potentials were not measured, the measured soil water contents were employed to calculate the volumetric water contents using the mea-

sured bulk density, and the soil water characteristic curve was utilized to calculate the matric potential.

The soil property curve was derived by fitting the van Genuchten equation using the data from all three measurements of both the water content ratio and matric potential. The soil water characteristic curves were determined by fitting the van Genuchten equation with all three simultaneous measurements of the soil water content and matric potential to determine the parameters.

The van Genuchten equation [25] is:

$$\frac{\theta - \theta_r}{\theta_s - \theta_r} = \frac{1}{[1 + (\alpha h)^n]^m}, \quad (2)$$

where θ is the volumetric water content [cm^3/cm^3], θ_r is the residual water content [cm^3/cm^3], θ_s is the saturated water content [cm^3/cm^3], h is the soil matrix potential [cmH_2O], α is a parameter corresponding approximately to the inverse of the air-entry value [cm^{-1}], and m and n are empirical shape-defining parameters. m is calculated as:

$$m = 1 - \frac{1}{n}. \quad (3)$$

The parameters were determined with the nonlinear least squares' method using the solver add-in in Excel for Microsoft 365. The initial values of θ_r and θ_s were set to 0.01 and 0.45, respectively, referring to the values of the soil parameters at locations close to our study sites [26].

2.5. Determination of Root Zone Depth

The root zone depth for each study sites was determined from the temporal variation of the depth distribution of the soil water content. In this study, we defined the "root zone" as the main depth at which plant roots could uptake water and nutrients for growth.

Therefore, in the root zone, which is affected by rainfall and evapotranspiration, the temporal changes in soil water content are large, whereas below the root zone, the temporal changes in soil water content are not so large. In this study, the root zone depth was determined from the temporal variation of the soil water content throughout the study period at each study site.

2.6. Calculation of the Average Matric Potential

The average matric potentials in the root zone and below the root zone at each study site were calculated as follows:

$$\Phi_{m,z} = \frac{\sum(\varphi_{m,i} \times d_i)}{\sum d_i}, \quad (4)$$

where $\Phi_{m,z}$ is the average matric potential at depth z , $\varphi_{m,i}$ is the matric potential at depth i , and d_i is the soil layer length at depth i . For example, when the root zone is 0–30 cm deep, the average matric potential in the root zone is given by

$$\Phi_{m,0-30 \text{ cm}} = \frac{(\varphi_{m,0-10 \text{ cm}} \times 10) + (\varphi_{m,10-20 \text{ cm}} \times 10) + (\varphi_{m,20-30 \text{ cm}} \times 10)}{30}. \quad (5)$$

2.7. Analysis of Soil Water Storage

To determine the amount of soil water storage, the soil water content at each depth was first multiplied times the bulk density to determine the volumetric water content. Then, this value was multiplied times the length to obtain the soil water storage at each depth. The soil water storage values at each depth were then summed to obtain the total soil water storage:

$$SWS_z = \sum(w_{c,i} \times \rho_{b,i} \times d_i), \quad (6)$$

where SWS is the total soil water storage at depth z , and $\rho_{b,i}$ is the bulk density at depth i . For example, the soil water storage at a depth of 0–30 cm is given by

$$SWS_{0-30 \text{ cm}} = (w_{c,0-10 \text{ cm}} \times \rho_{b,0-10 \text{ cm}} \times 10) + (w_{c,10-20 \text{ cm}} \times \rho_{b,10-20 \text{ cm}} \times 10) + (w_{c,20-30 \text{ cm}} \times \rho_{b,20-30 \text{ cm}} \times 10). \quad (7)$$

2.8. Evaluation of Soil Water Storage Effect during Fallow Period

The effect of soil water storage during the fallow period was evaluated in two ways: (i) by calculating the precipitation storage efficiency (PSE) and (ii) by assessing the difference between the soil water storage in the field after the fallow period and that in the adjacent rangeland.

PSE is the fraction of precipitation that falls in a given time period that is stored in the soil profile and is given by

$$PSE(\%) = 100 \times \left(\frac{SWS_{0-60 \text{ cm}}^Y - SWS_{0-60 \text{ cm}}^{Y-1}}{P^Y} \right), \quad (8)$$

where $SWS_{0-60 \text{ cm}}^Y$ and $SWS_{0-60 \text{ cm}}^{Y-1}$ are the average soil water storage at a depth of 0–60 cm measured 2–4 times at each study site in the autumn of years Y and $Y - 1$. P^Y is the amount of precipitation from the time of the fall survey in year $Y - 1$ to the time of the fall survey in year Y and this is approximately equal to the annual precipitation in year Y . P^Y was obtained at weather station in Hustai National Park located 11–13 km southeast of the study sites (Table 2).

The difference between the soil water storage in the field after the fallow period and the soil water storage in the adjacent rangeland (DSWS) was calculated as:

$$DSWS(\%) = 100 \times \left(\frac{SWS_{0-60 \text{ cm}}^Y(\text{Field}) - SWS_{0-60 \text{ cm}}^Y(\text{Rangeland})}{P^Y} \right) \quad (9)$$

where $SWS_{0-60 \text{ cm}}^Y(\text{Field})$ is $SWS_{0-60 \text{ cm}}^Y$ in FR or FW and $SWS_{0-60 \text{ cm}}^Y(\text{Rangeland})$ is $SWS_{0-60 \text{ cm}}^Y$ in RR or RW. The following equation was used to determine DSWS in FR:

$$DSWS(\%) = 100 \times \left(\frac{SWS_{0-60 \text{ cm}}^Y(\text{FR}) - SWS_{0-60 \text{ cm}}^Y(\text{RR})}{P^Y} \right), \quad (10)$$

and the DSWS in FW was calculated as follows:

$$DSWS(\%) = 100 \times \left(\frac{SWS_{0-60 \text{ cm}}^Y(\text{FW}) - SWS_{0-60 \text{ cm}}^Y(\text{RW})}{P^Y} \right). \quad (11)$$

3. Results

3.1. Soil Water Characteristic Curves

Figure 5 shows the relationships between the matric potential and water content directly measured in August 2016, April 2017, and June 2018 at all study sites. The root zones are 0–30 cm deep at all the study sites, which will be discussed in detail in Section 3.2. The relationship between the matric potential and soil water content was expressed separately in the root zone (0–30 cm depth) and below the root zone (30–60 cm depth). After fitting the van Genuchten equation to the relationship between the matric potential and soil water content, the results reveal almost the same relationship between FR and FW and between RR and RW. Therefore, the same equations were used for FR and FW and for RR and RW, respectively. Table 3 shows the parameters in each van Genuchten equation (Equation (2)).

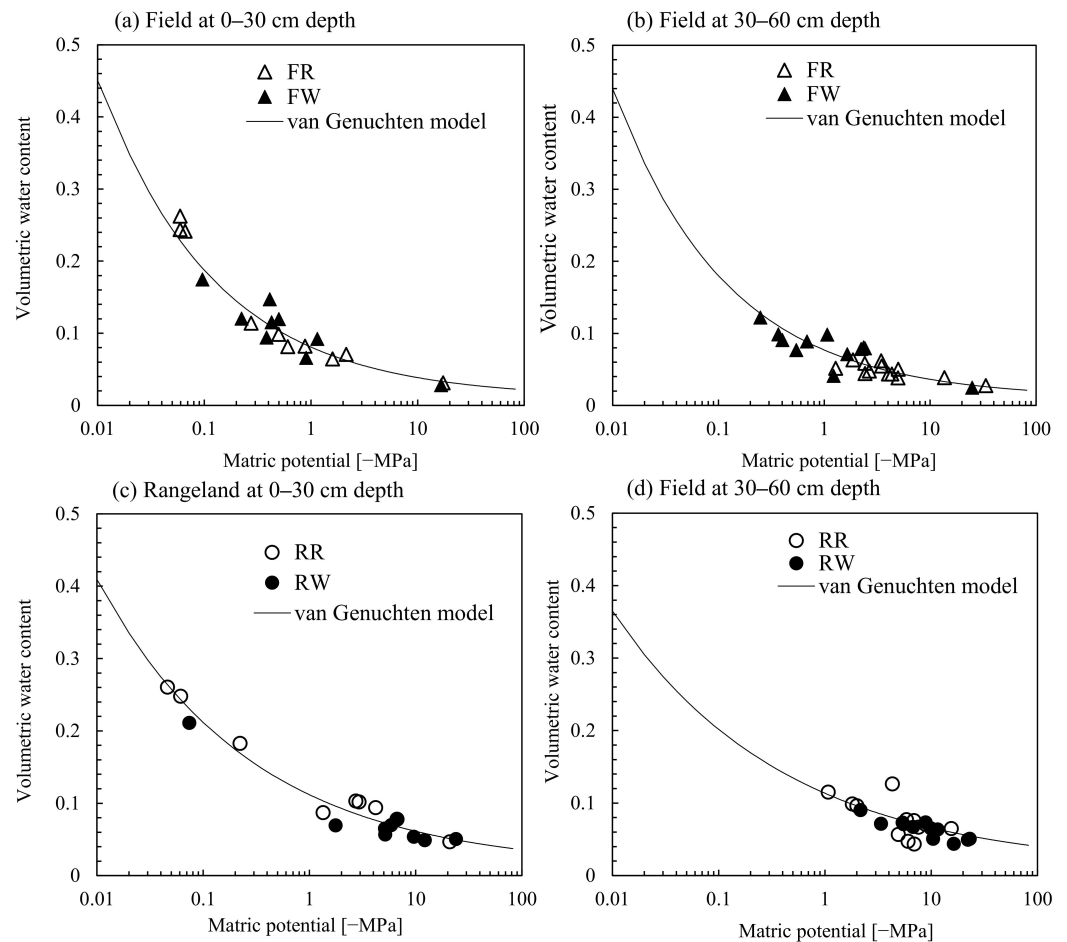


Figure 5. Relationships between the matric potential and water content, which were measured in August 2016, April 2017, and June 2018 (a) at 0–30 cm depth and (b) 30–60 cm at two field sites, the FR and FW, and (c) at 0–30 cm depth and (d) 30–60 cm at two rangeland sites, RR and RW.

Table 3. Parameters of the van Genuchten model used in Equation (2).

Site	Depth	Parameters				
		θ_r [cm ³ /cm ³]	θ_s [cm ³ /cm ³]	α [cm ^{−1}]	n [–]	m [–]
Rangelands (RR, RW)	0–30 cm	0.01	0.491	0.0184	7.49	0.04
Rangelands (RR, RW)	30–60 cm	0.01	0.491	0.0308	7.01	0.038
Fields (FR, FW)	0–30 cm	0.01	0.495	0.0121	7.23	0.055
Fields (FR, FW)	30–60 cm	0.01	0.491	0.0128	8.01	0.05

3.2. Determination of the Root Zone Depth

Figures 6 and 7 show the vertical distributions of soil water contents and matric potential between October 2015 and April 2017 and between October 2017 and August 2019, respectively. The chain lines in the matric potential figures represent the permanent wilting point (PWP; –1.55 MPa). In addition, the vertical distributions of the bulk density are shown in Figure 8. In FR, the bulk density could only be measured up to a depth of 50 cm owing to the drying of the soil. However, the bulk density at a depth of 50–60 cm was assumed to be unaffected by tillage and used the bulk density at a depth of 50–60 cm in the adjacent RR as a proxy. The matric potential was calculated from the soil water content using the soil water characteristic curve, except in August 2016, April 2017, and June 2018.

The soil water content and matric potential at a depth of 0–30 cm varied greatly among the sampling days from 0.02 to 0.27 g/g and from -24 to -0.04 MPa at all sites (Figures 6 and 7). The soil water contents below a depth of 30 cm were low and remain almost constant regardless of the depth and time ranging from 0.02 to 0.1 g/g at all sites except RR after October 2017 (Figures 6 and 7). Therefore, the root zone was defined to have a depth range of 0–30 cm, where the change in the soil water content was large at all study sites. The two soil water content distributions sampled in RR on 28 October 2017 were distinctly different, 0.14 and 0.22 g/g, at a depth of 30–60 cm (Figure 7b). Afterwards, in October, the two soil water contents below the root zone collected on the same day in RR differ considerably.

3.3. Temporal Changes in Soil Water Storage and Matric Potential at the Study Sites

Figure 9 presents the average soil water storage at depths of 0–30 cm, 30–60 cm, and 0–60 cm for each survey period at all study sites. The soil water storage in the root zone layer (0–30 cm depth) varied greatly, lying in the ranges of 20–55, 26–64, 26–48, and 19–48 mm in FR, RR, FW, and RW, respectively. The soil water content below the root zone varied slightly in the range of ± 10 mm (with range of 14–26, 22–24, 21–29, and 18–26 mm in FR, RR, FW, and RW, respectively), except in RR after October 2017 and RW in October 2017. The soil water storage at a depth of 0–60 cm in RR in October 2017 was remarkably larger (=133 mm) than that at the other sites (=48–76 mm) at that time (Figure 9).

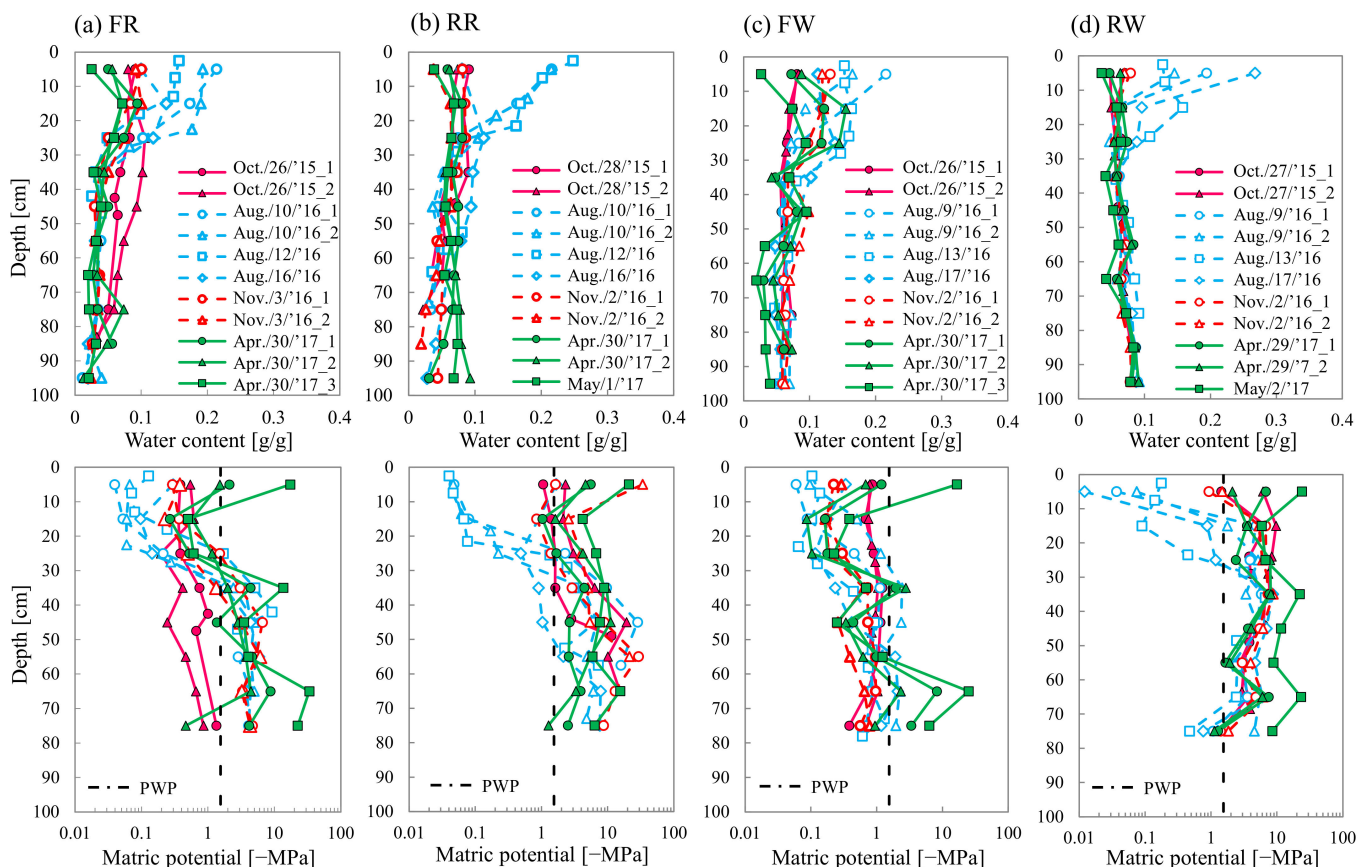


Figure 6. Temporal changes in soil moisture with time. The figures above show the vertical distributions of water content; the others below show that of water potential at (a) FR, (b) RR, (c) FW, and (d) RW in 2015 and 2016. The dashed line represents the permanent wilting point (PWP; -1.55 MPa). FR is the rapeseed field, FW is the wheat field, RR is the rangeland adjacent to FR, and RW is the rangeland adjacent to FW. According to the weather station located 11–13 km southeast of the study sites, no rain and snow was observed in the weeks preceding 2 November 2016 and 29 April 2017 and rain or snow was observed on 25 October 2015 (=3.5 mm) and August 9 and 10 (=25 and 39 mm, respectively), 2016. We confirmed snowing and snow pile-up on-site on 25 October 2015 and heavy rainfall on 10 August 2016.

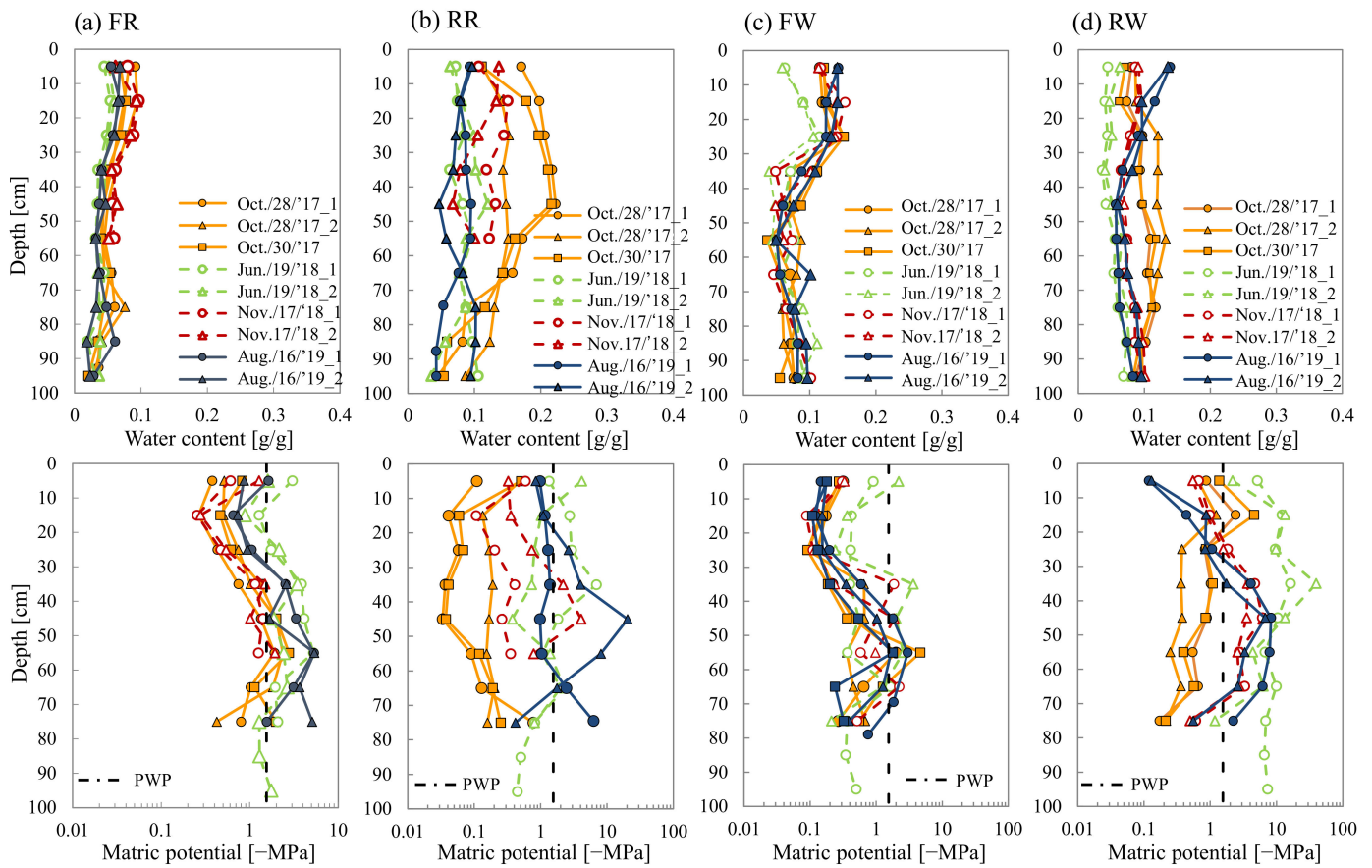


Figure 7. Temporal changes in soil moisture with time. The figures above show the vertical distributions of water content; the others below show that of water potential at (a) FR, (b) RR, (c) FW, and (d) RW in 2017–2019. The dashed line represents the permanent wilting point (PWP; -1.55 MPa). FR is the rapeseed field, FW is the wheat field, RR is the rangeland adjacent to the FR, and RW is the rangeland adjacent to the FW. According to the weather station located 11–13 km southeast of the study sites, no rain and snow was observed in the week preceding 17 November 2018, and rain or snow was observed on 27 October 2017 ($=0.5$ mm) and 17 June 2018 ($=7$ mm). We confirmed mottled snow on 28 October 2017 and slight rainfall on 13 August 2019. Moreover, the soil was frozen and very hard on 17 November 2018.

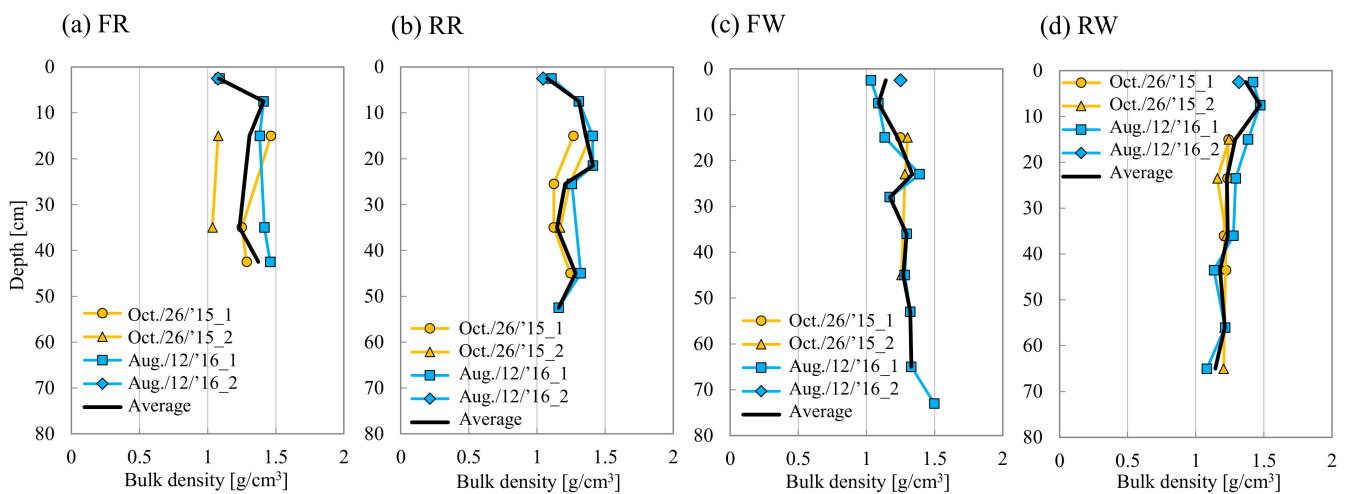


Figure 8. Vertical distributions of bulk density at (a) FR, (b) RR, (c) FW, and (d) RW.

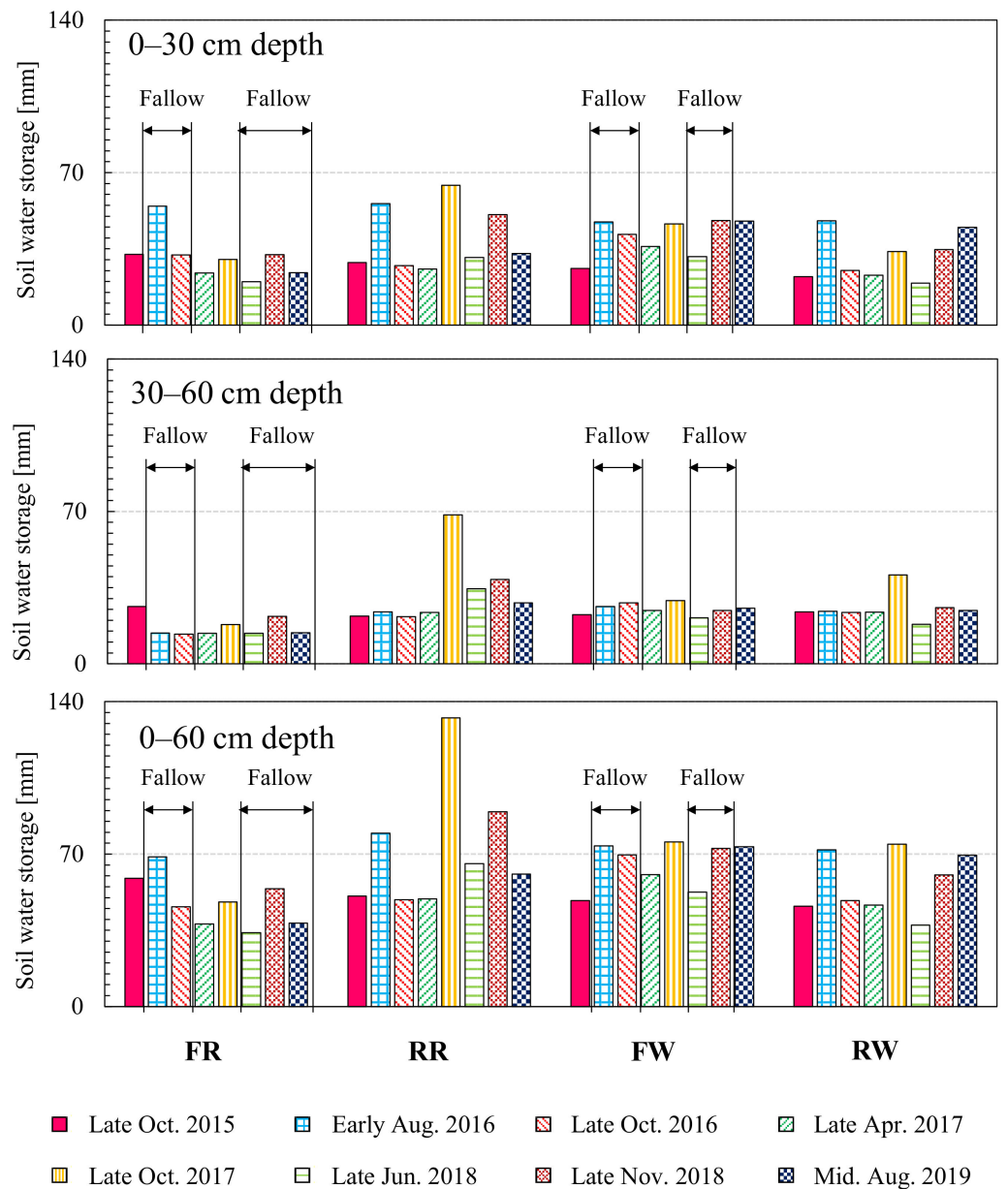


Figure 9. Changes in soil water storage in the root zone (0–30 cm depth), below the root zone (30–60 cm depth), and in the depth of 0–60 cm at the study sites from 2015 to 2019. FR is the rapeseed field, RR is the rangeland adjacent to FR, FW is the wheat field, RW is the rangeland adjacent to FW. “Fallow” indicates as fallow year in FR and FW.

Figure 10 shows the differences in soil water storages between the fields and rangelands in the root zone (0–30 cm depth), below the root zone (30–60 cm depth), and at a depth of 0–60 cm, which were calculated by subtracting the soil water storage levels in the adjacent to adjacent rangelands from those of the fields. However, the soil water storage in RW was used instead of that in RR for calculating the difference in soil water storage between FR and RR after October 2017 because the soil water storage in RR was affected by heavy precipitation in October 2017.

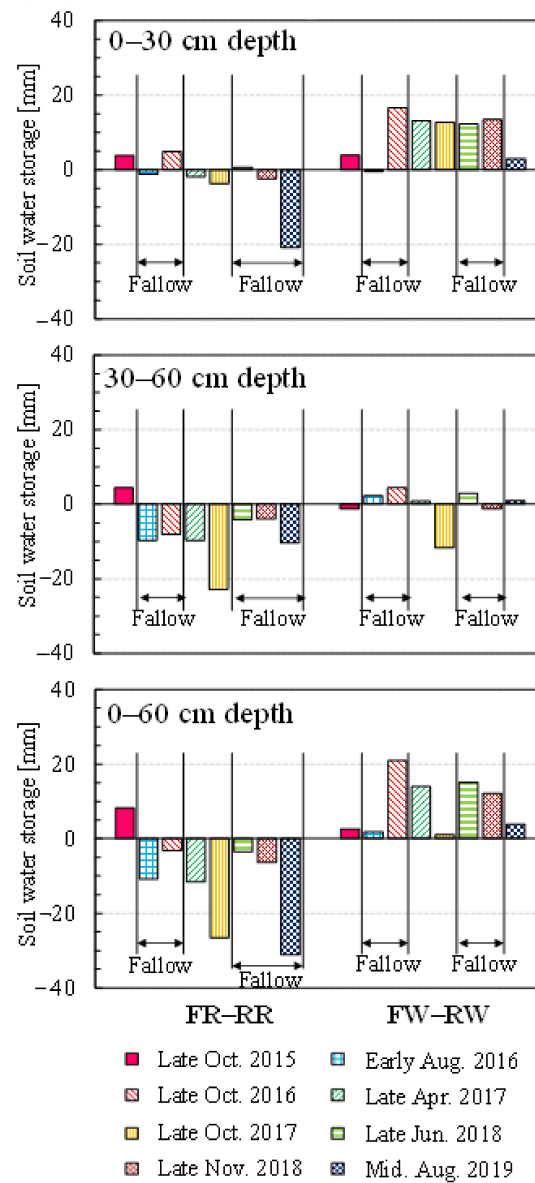


Figure 10. Differences in soil water storage between the fields and rangelands in the root zone (0–30 cm depth), below the root zone (30–60 cm depth), and in the depth of 0–60 cm in the study sites, which were calculated by subtracting the soil water storage in the adjacent rangelands from that in the fields. RW was used instead of RR for FR–RR calculations after October 2017 because RR had considerably higher infiltration than the other sites due to surface inflow from the adjacent road, which continued until 2019. FR is the rapeseed field, FW is the wheat field, RR is the rangeland.

In accordance with the crop production history (Table 2), Figure 10 indicates that the water storage in the root zone in FR was only -4 to 5 mm larger than that in RR regardless of whether the year was a fallow or production year, except in August 2019 (fallow season) when the soil water storage in FR was 21 mm less than that in RR. The soil water storage at a depth of 0–60 cm in FR was 4 – 23 mm less than that in RR except in October 2015 when the soil water storage in FR in October 2015 was 4 mm greater than that in RR.

The water storage in the root zone in FW in the production years (except in October 2017) was only 3 – 4 mm larger than that in RW; however, the water storage in FW in the fallow years (except in August 2016) was clearly 12 – 17 mm larger than that in RW. The water storage in FW in October 2017 was 13 mm larger than that in RW, whereas it was the same as that in RW in August 2016. The water storage at a depth of 0–60 cm in FW was only 1 – 4 mm larger than that in RW in the production years and clearly 12 – 21 mm

larger than that in RW in the fallow years, except in August 2016. The water storage in FW in August 2016 was only 2 mm larger than that in RW. Furthermore, the water storage at depths of 0–60 cm in FW in the production years was almost the same as that in RW and clearly 12–21 mm larger than that in RW in the fallow years, except in August 2016 and October 2017. The soil water storage in the root zone in FW in August 2016 was almost the same as that in RW despite being a fallow year because the field was filled with weeds before plowing, and the weeds may have absorbed large quantities of soil water. The soil water storage in the root zone in FW in the production years was larger than that in RW, whereas it was smaller under the root zone in October 2017. However, the soil water storage at a depth of 0–60 cm was almost the same as that in RW (Figure 10).

Figure 11 shows the average matric potentials in the root zone (0–30 cm depth) and below the root zone (30–60 cm depth) for each survey period at all study sites. The matric potential in the root zone of the soil samples just after rain or snow, i.e., in October 2015, August 2016, October 2017, and August 2019, was approximately the same as or wetter than that at the PWP, except in RR and RW in October 2015. The matric potential in the root zone of the soil samples when no rain or snow was observed in the week preceding soil sampling, i.e., November 2016 and April 2017, was drier than that at the PWP, except in RR and RW in November 2016. The matric potential below the root zones in FR, RR, and RW was always almost drier than the PWP; however, the matric potential of FW was almost the same or slightly wetter (Figure 11).

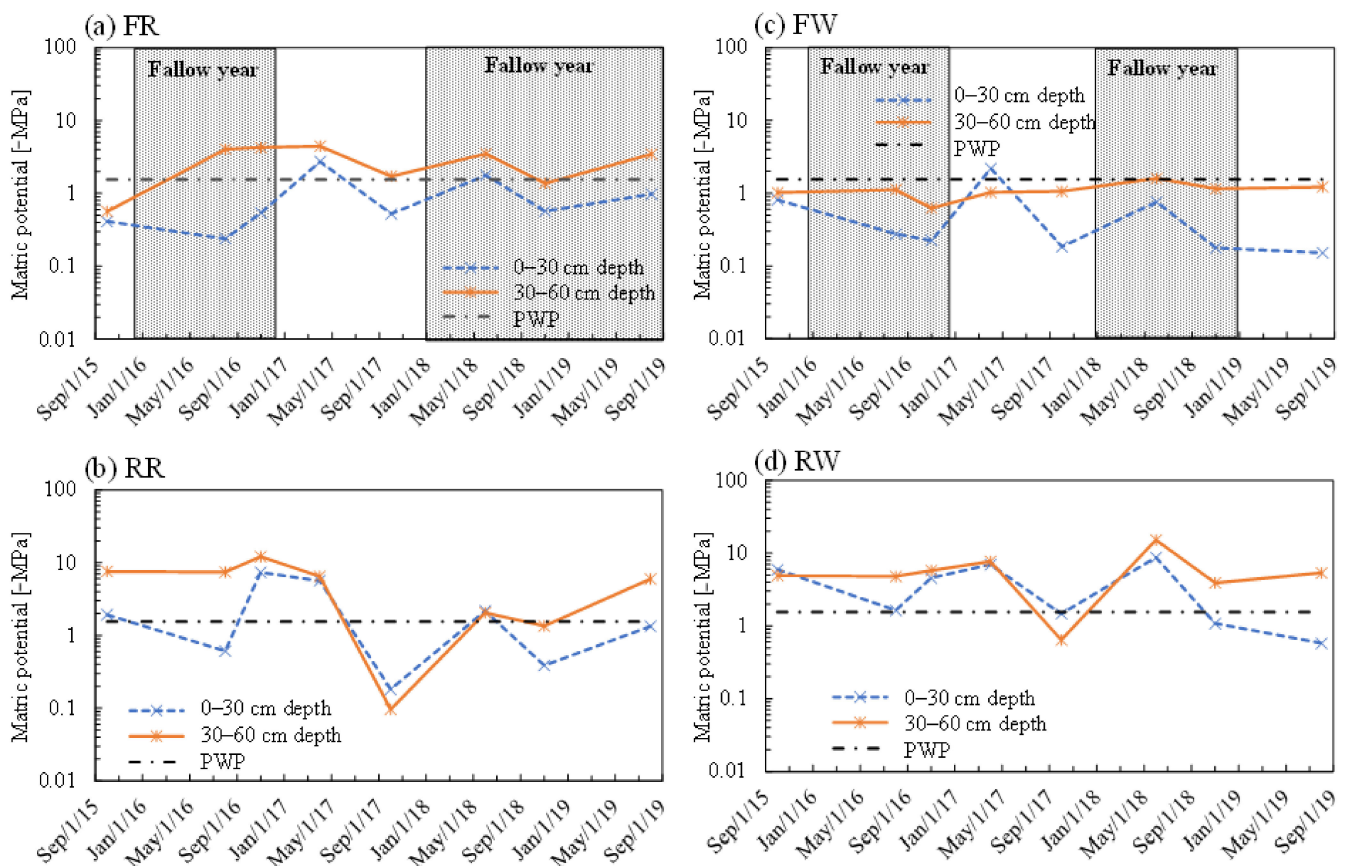


Figure 11. Change in average matric potential in the root zone (0–30 cm depth) and below the root zone (30–60 cm depth) at (a) FR, (b) RR, (c) FW, and (d) RW from 2015 to 2019. The dashed lines represent the permanent wilting point (PWP; -1.55 MPa). FR is the rapeseed field, FW is the wheat field, RR is the rangeland adjacent to FR, and RW is the rangeland adjacent to FW.

3.4. Soil Water Storage Effects during the Fallow Period

Table 4 shows *PSE* from 2016 to 2018 and *DSWS* from 2015 and 2018. *PSE* in *FW* shows an 11% soil water storage effect in the fallow year of 2016 but no effect of soil water storage in the fallow year of 2018. Additionally, there was no effect of soil water storage in the production year of 2017. In *DSWS*, no effect of soil water storage was observed in the production years of 2015 and 2017, whereas 6–11% soil water storage effects were observed in the fallow years of 2016 and 2018.

Table 4. The results of the precipitation storage efficiency (*PSE*) and the difference between the soil water storage in a field after fallow period and the soil water storage in adjacent rangeland (*DSWS*).

	Year	Field State	FR	FW
<i>PSE</i> (%)	2016	F	−6.8	10.9
	2017	P	1.2	3.3
	2018	F	2.8	−1.4
<i>DSWS</i> (%)	2015	P	4.6	1.5
	2016	F	−1.7	10.9
	2017	P	−14.6	0.6
	2018	F	−2.9	5.6

The *PSE* in *FR* did not demonstrate a soil water storage effect in either the production or fallow years, and the *DSWS* exhibited no soil water storage effect in the fallow years. The autumn 2017 survey was assumed to be affected by rain. Therefore, the *PSE* in *FW* in 2018 was −1% and the effect of soil water storage could not be evaluated. In such cases, the use of *DSWS* is preferred.

4. Discussion

4.1. Soil Water Storage in the Rangelands

In the rangelands, the soil water content and matric potential below the root zone were usually almost constant regardless of the depth, and were drier than the *PWP*, with a few exceptions such as when large amounts of rainwater or snowmelt suddenly infiltrated the soil owing to heavy rain or snowmelt (Figures 6 and 7). Miyazaki et al. [27] reported that in the Mongolian steppe, where the annual precipitation and annual mean air temperature are 245 mm and 0.4 °C, respectively, and the soil type of the soil surface is brown humus sand, the soil water content below 40 cm depth changes only slightly, and 79–94% of the annual precipitation is lost from the soil as evapotranspiration. Yamanaka et al. [19] reported that the total precipitation and evapotranspiration from June to August were almost equal and rainfall water did not infiltrate below 20 cm depth on four steppes with annual precipitation of around 100 mm and mean temperatures of around 0 °C, where the soil is sandy loam or sandy silt loam with abundant gravel. Therefore, rainwater increases the soil water content in the root zone only, rarely reaching below the root zone. Moreover, the soil water in the root zone immediately after rainfall is lost owing to evapotranspiration.

The nonuniform soil water distributions in *RR* in October 2017 (Figure 7) suggest that large amounts of water ponding may have occurred at this site. Miyasaka et al. [28] reported that the horizontally nonuniform water content distributions are caused by water ponding because the rainfall intensity is sometimes greater than the infiltration rate. Further, the large water ponding may have been caused by the surface outflow from an adjacent road, which was not paved but rather compacted by vehicles into the rangeland. Therefore, the nonuniform water distributions in *RR* were attributed to the large water ponding; at the other sites, water ponding may not have occurred. The occurrence of large water ponding in only *RR* is not attributed to the considerably greater rainfall intensity relative to the infiltration rate of the soil surface in *RR*, but rather to the surface flow in the adjacent road, where the infiltration rate may be considerably lower than the rainfall intensity. A reason for this inference is that the soil water storage at depths of 0–60 cm in *FR* and

FW in October 2017 was considerably lower than that in RR (Figure 9), although all of the rainwater infiltrated the soil in the croplands where the infiltration rates were considerably higher than those in the rangeland because of appropriate cultivation. The second reason is that a nonuniform water distribution was not observed in RW, where the infiltration rate and rainfall intensity were almost the same as those in RR. The third reason is that RR was located near a road, but the other sites were not close to roads.

4.2. Soil Water Storage in Wheat and Rapeseed Field

Both wheat and rapeseed are known to have deep root elongation in both crops [29]. Comparing the root depth of rapeseed and wheat under almost the same climatic, soil, and management conditions, it has been reported that there was no significant difference between the two crops [30,31]. According to Gan et al. [30], the percentage of roots above 40 cm depth was 67% for spring wheat and 58% for rapeseed, and above 60 cm depth was 88% for spring wheat and 82% for rapeseed in a pot-study. According to Cutforth et al. [31], the percentage of roots above 40 cm depth was about 64% for spring wheat and about 60% for rapeseed and above 60 cm depth was 80% for spring wheat and 75% for rapeseed in field study, and the root mass for rapeseed was lower than wheat in the soil layers above the 60 cm depth but steadily increased for depths below 60 cm so that rapeseed had the highest root mass in the 100–120 cm layer. On the other hand, in Mongolian steppe plants, about 80% of the root weight is concentrated at a depth of up to 20 cm, with the deepest roots reaching only 50 cm at most [32]. Therefore, field crops will develop deeper roots than rangeland plants, although root depth depends on soil properties and climatic conditions. However, the temporal changes in the soil water content distributions in the fields were similar to those in the rangelands, suggesting that little precipitation percolated below the root zone and that most of the precipitation was lost by evapotranspiration (Figures 6 and 7).

Although rainfall that percolates below the root zone occurs only once to a few times a year [28,33], the difference in the matric potential below the root zone between wheat and rapeseed fields will be due to the difference in water absorption by roots extending deeper than the root zone.

Plant growth refers to photosynthesis, the production of organic matter using carbon dioxide, water and solar radiation energy. In order to take in the carbon dioxide needed for photosynthesis from the atmosphere, it is necessary to open the many stomata in the leaves. When the stomata are opened, plants' water evaporates from the stomata and is lost. Plant growth refers to photosynthesis, the production of organic matter using carbon dioxide, water and solar radiation energy. In order to take in the carbon dioxide needed for photosynthesis from the atmosphere, it is necessary to open the many stomata in the leaves. When the stomata are opened, plants water evaporates from the stomata and is lost. When the soil becomes dry and the plant is unable to absorb enough water through its roots, the amount of water lost through transpiration from the stomata exceeds the amount of water absorbed, and the water in the plant body decreases. As a result, the swelling pressure in the plant cells also decreases. Although the decrease in swelling pressure closes the stomata and reduces the rate of photosynthesis [34], thereby inhibiting further water loss, the plant will die permanently if this condition continues. To avoid such die-off, plants are known to have developed various drought tolerances [35,36].

When the soil water decreases and the plant is unable to absorb sufficient water, wheat is thought to close its stomata at a higher moisture state than rapeseed, preventing water loss in the plant. On the other hand, rapeseed does not close its stomata even when the soil is dry above the PWP, which is thought to maintain the expansion pressure of plant cells and photosynthesis. Merrill et al. [37] found seasonal soil water use was dependent on seasonal precipitation with the average soil water use tending to be highest for rapeseed, intermediate for spring wheat, and least for dry pea. Moreover, they found that rapeseed withdrew about 45% of the water used from a depth of 60 cm or less, while wheat withdrew 33% of the water used from a depth of 60 cm or less in a year with low precipitation.

Gan et al. [38] reported that water use for rapeseed was similar to wheat in a semiarid environment. In the present study, area, there was little difference in soil water storage between FR and FW, but there was a large difference in the value of matric potential. Therefore, it is difficult to reveal small differences in the amount of water use by plants based on changes in root length/weight and water storage, suggesting the importance to measure matric potential by depth.

The comparison of the effects of soil water storage during the fallow year between FR and FW showed that *PSE* in 2016 was 11% for FW and -7% for FR. The *DSWS* results in 2016 and 2018 were similar. Previous scholars have reported a 16-month fallow *PSE* of 11% (ranging from 1–18%) in the Segarra region in Spain [21], a 14-month fallow *PSE* of 20% (ranging from 8–34%) in the Great Plains [22], and a 14–21-month fallow *PSE* of approximately 25% (ranging from 10–37%) in the Great Plains [23].

Although the amount of the stock of soil water storage during the fallow period is affected by the soil type, cropping system, and management [39], the *PSE* of the wheat fields during the fallow year in this study was within the range of values of these previous studies. On the other hand, the *PSE* of the rapeseed fields during the fallow year in this study was significantly smaller than the values of these previous studies.

It is possible that some weeds were growing in the field before plowing, which may have absorbed some quantities of soil water in the summer during the fallow year. Moreover, the possible causes for not storing soil water during the fallow period in the rapeseed field may be the high rapeseed seed losses at the time of harvest.

Figure 12a shows the photographs during plowing at FW, the right and left sides correspond to before and after plowing, respectively. Before plowing, short weeds were sparsely growing in the field. While Figure 12b shows during plowing at FR, the upper and bottom sides correspond to before and after plowing, respectively. Before plowing, tall weeds were densely growing in the field. These weeds may have grown from the rapeseed spilled in the previous year. These weeds may use almost all the soil water in FR in fallow fields.



Figure 12. Photographs of (a) FW and (b) FR, which were plowed in mid-August 2016.

Rapeseed is subject to significant losses at harvest time, due to both natural shedding and mechanical harvesting operations [40]. Therefore, many volunteer rapeseeds will germinate the year after harvesting [41], and the volunteer rapeseeds will use the soil water storage.

Measures to increase water storage during fallow periods due to rapeseed production include the introduction of machinery suitable for rapeseed harvesting, the use of no-till and chemical fallow systems and increased tillage frequency. Farmers using unsuitable wheat harvesting machineries previously observed significant leakage of rapeseed, which germinated the next year [11]. Therefore, farmers should use suitable harvesting machineries for rapeseed. Pari et al. [42] showed that the seed loss reduction achieved by employing rapeseed combine headers (a decrease in loss of 0.97% of the total production) is lower than

that resulting from using wheat combine headers (1.63% of the total production) during the harvesting of rapeseed.

5. Conclusions

In this study, we focused on soil water conditions in wheat and rapeseed fields and demonstrated the effects of agricultural production on the soil water conditions in the rangeland. The soil water content and matric potential were measured in wheat and rapeseed fields, as well as two rangelands adjacent to these fields.

The results of this study demonstrate that the matric potential below the root zone of the rapeseed field and two rangelands were almost drier and that of the wheat field was wetter than the PWP all year. These results suggest that wheat uses less water than Mongolian rangeland plants, and rapeseed uses almost all the water available to the plants, similar to the rangeland plants.

In addition, fields left fallow after wheat harvesting had 12–21 mm more soil water storage than the adjacent rangelands, equivalent to 5–10% of the annual precipitation. On the other hand, in the rapeseed field, the soil water storage was about the same as in the adjacent rangeland, and there was no increase in soil water storage during the fallow year. This characteristic may be due to the fact that many seeds were spilled during harvesting and many rapeseeds germinated the following year, absorbing most of the soil water.

In arid areas where water, which is essential for plant growth, is low initially, rapeseed production further reduces the amount of water in the soil, which is one of the reasons that Mongolian farmers are concerned about rapeseed production degrading the land.

Author Contributions: Conceptualization, K.M. and T.M.; data curation, K.M. and J.O.; funding acquisition, K.M. and T.M.; investigation, K.M., T.M., J.O., S.B. and U.J.; methodology, K.M. and T.M.; project administration, K.M. and T.M.; visualization, K.M. and J.O.; writing—original draft preparation, K.M.; writing—review and editing, K.M. All authors have read and agreed to the published version of the manuscript.

Funding: This work was financially supported by Grant-in Aid for Young Scientists (B) (No. 15K18818) and “Researcher Dispatch” Program in 2017 from Regional Research Institute of Agricultural Production, College of Bioresource Sciences, Nihon University.

Institutional Review Board Statement: Not applicable.

Informed Consent Statement: Not applicable.

Data Availability Statement: All data are provided in the manuscript.

Acknowledgments: We sincerely thank Hustai National Park for their cooperation. We would also like to thank the staff at the Mongolian University of Life Sciences for their cooperation.

Conflicts of Interest: The authors declare no conflict of interest.

Appendix A

Because the study site did not have an oven, the “gas stove method” was adopted to measure the soil water content using a gas stove. In the gas stove method, the soil water content can be measured by directly heating a container containing a soil sample.

First, the soil sample was placed in an aluminum container and the wet weight of the soil was measured. Next, the aluminum container with the sample was placed in a frying pan and the pan was covered with a lid. The pan was then heated on a gas stove. Using an infrared thermometer, the soil moisture was evaporated under low heat for approximately 1 h until the surface temperature of the soil sample exceeded 110 °C. The weight of the soil sample after heating (dry soil weight) was measured, and the moisture content ratio was calculated using Equation (1).

The gas stove method was compared and validated with the oven drying method (ISO 17892-1:2014), which is commonly used for soil water content measurement. The soil samples were stirred well to obtain a uniform soil water content and placed in six aluminum

containers of 20–40 g each. Three soil samples were measured using the gas stove method and oven drying method, and the results were compared. Two types of soil samples, namely sand dune sand and sandy clay loam, were used. Two types of soil water contents were prepared for each soil, namely wet and dry.

Table A1 presents the results. Although the soil water content measured using the gas stove method was 0–0.01 g/g higher than that measured using the oven drying method, it was almost within the error range. Therefore, the gas stove method can be regarded as equivalent to the oven drying method.

Table A1. Measurement results of gas stove method and oven drying method. M_w : mass of moist soil (g); M_d : mass of dried soil (g); w_c : gravimetric soil water content (g/g).

Soil	Gas Stove Method			Oven Drying Method			
	M_w	M_d	W_c	M_w	M_d	W_c	
Sand dune sand	wet 1	39.35	33.34	0.18	31.07	26.57	0.17
	wet 2	35.54	30.21	0.18	34.99	29.87	0.17
	wet 3	35.36	29.96	0.18	39.46	33.57	0.18
	Average			0.18			0.17
	dry 1	36.23	34.99	0.04	35.32	34.16	0.03
	dry 2	29.00	28.01	0.04	30.01	29.00	0.03
	dry 3	33.55	32.40	0.04	32.61	31.52	0.03
	Average			0.04			0.03
Sandy clay loam	wet 1	21.55	18.51	0.16	18.33	15.77	0.16
	wet 2	17.39	14.96	0.16	24.53	21.11	0.16
	wet 3	21.98	18.87	0.16	15.11	13.01	0.16
	Average			0.16			0.16
	dry 1	17.61	16.83	0.05	23.38	22.39	0.04
	dry 2	22.71	21.72	0.05	25.60	24.52	0.04
	dry 3	24.60	23.52	0.05	25.16	24.10	0.04
	Average			0.05			0.04

References

1. Mongolian Statistical Information Service. Mongolian Statistical Yearbook. 2020. Available online: <http://www.1212.mn> (accessed on 1 May 2020).
2. Didier, K.; Lkhamjav, O. *The Potential for Intensive Crop Production in the Eastern Steppe of Mongolia: History, Current Status, Government Plans, and Potential Impacts on Biodiversity*; USAID: Washington, DC, USA, 2009. Available online: <https://programs.wcs.org/databases/doi/ctl/view/mid/33065/pubid/DMX540100000.aspx> (accessed on 5 March 2021).
3. Erdenebolor, B.; Nyamgerel, B. *Value Chain Analysis of Wheat, Potato and Rapeseed in Mongolia*; Federal Ministry of Food and Agriculture: Bonn, Germany, 2017.
4. Grami, B.; Lacroix, L.J. Cultivar variation in total nitrogen uptake in rape. *Can. J. Plant Sci.* **1977**, *57*, 619–624. [[CrossRef](#)]
5. Svecnjak, Z.; Rengel, Z. Canola cultivars differ in nitrogen utilization efficiency at vegetative stage. *Field Crops Res.* **2006**, *97*, 221–226. [[CrossRef](#)]
6. Ye, X.S.; Hong, J.A.; Shi, L.; Xu, F.S. Adaptability mechanism of nitrogen-efficient germplasm of natural variation to low nitrogen stress in *Brassica napus*. *J. Plant Nutr.* **2010**, *33*, 2028–2040. [[CrossRef](#)]
7. Stanhill, G. Water-use efficiency. *Adv. Agron.* **1986**, *39*, 53–85.
8. Zhang, H.; Turner, N.C.; Poole, M.L. Yield of wheat and canola in the high rainfall zone of south-western Australia in years with and without a transient perched water table. *Aust. J. Agric Res.* **2004**, *55*, 461–470. [[CrossRef](#)]
9. Hu, Q.; Hua, W.; Yin, Y.; Zhang, X.K.; Liu, L.J.; Shi, J.Q.; Zhao, Y.G.; Qin, L.; Chen, C.; Wang, H.Z. Rapeseed research and production in China. *Crop J.* **2017**, *5*, 127–135. [[CrossRef](#)]
10. Faghih, H.; Behmanesh, J.; Rezaie, H.; Khalili, K. Climate and rainfed wheat yield. *Theor. Appl. Climatol.* **2021**, *144*, 13–24. [[CrossRef](#)]
11. Orgil, B. *Towards Stronger Rapeseed Policy as a Cash Crop in Mongolia*; CDN Policy Oriented Research Paper; Cooperation and Development Network of Pavia: Pavia, Italy, 2017. Available online: http://www.cooperationdevelopment.org/wp-content/uploads/2018/01/POR_CDN-Policy-research-paper-Orgil-Balgansuren.pdf (accessed on 5 March 2021).
12. Yang, C.; Geng, Y.; Fu, X.Z.; Coulter, J.A.; Chai, Q. The effects of wind erosion depending on cropping system and tillage method in a semi-arid region. *Agronomy* **2020**, *10*, 732. [[CrossRef](#)]

13. Sankey, T.T.; Massey, R.; Yadav, K.; Congalton, R.G.; Tilton, J.C. Post-socialist cropland changes and abandonment in Mongolia. *Land. Degrad. Dev.* **2018**, *29*, 2808–2821. [[CrossRef](#)]
14. Tian, F.; Herzschuh, U.; Mischke, S.; Schlutz, F. What drives the recent intensified vegetation degradation in Mongolia—Climate change or human activity? *Holocene* **2014**, *24*, 1206–1215. [[CrossRef](#)]
15. Wang, J.; Brown, D.G.; Chen, J.Q. Drivers of the dynamics in net primary productivity across ecological zones on the Mongolian Plateau. *Landsc. Ecol.* **2013**, *28*, 725–739. [[CrossRef](#)]
16. Yanagawa, A.; Sasaki, T.; Undarmaa, J.; Okuro, T.; Takeuchi, K. Factors limiting vegetation recovery processes after cessation of cropping in a semiarid grassland in Mongolia. *J. Arid Environ.* **2016**, *131*, 1–5. [[CrossRef](#)]
17. Zhao, W.Z.; Xiao, H.L.; Liu, Z.M.; Li, J. Soil degradation and restoration as affected by land use change in the semiarid Bashang area, northern China. *Catena* **2005**, *59*, 173–186. [[CrossRef](#)]
18. Liu, S.; Li, S.G.; Yu, G.R.; Asanuma, J.; Sugita, M.; Zhang, L.M.; Hu, Z.M.; Wei, Y.F. Seasonal and interannual variations in water vapor exchange and surface water balance over a grazed steppe in central Mongolia. *Agric. Water Manag.* **2010**, *97*, 857–864. [[CrossRef](#)]
19. Yamanaka, T.; Kaihotsu, I.; Oyunbaatar, D.; Ganbold, T. Summertime soil hydrological cycle and surface energy balance on the Mongolian steppe. *J. Arid Environ.* **2007**, *69*, 65–79. [[CrossRef](#)]
20. Lu, N.; Shen, S.; Wilske, B.; Sun, G.; Chen, J. Evapotranspiration and soil water relationships in a range of disturbed and undisturbed ecosystems in the semi-arid Inner Mongolia, China. *J. Plant Ecol.* **2011**, *4*, 49–60. [[CrossRef](#)]
21. Lampurlanes, J.; Angas, P.; Cantero-Martinez, C. Tillage effects on water storage during fallow, and on barley root growth and yield in two contrasting soils of the semi-arid Segarra region in Spain. *Soil Tillage Res.* **2002**, *65*, 207–220. [[CrossRef](#)]
22. Nielsen, D.C.; Vigil, M.F. Precipitation storage efficiency during fallow in wheat-fallow systems. *Soil Water* **2010**, *102*, 537–543. [[CrossRef](#)]
23. Peterson, G.A.; Schlegel, A.J.; Tanaka, D.L.; Jones, O.R. Precipitation use efficiency as affected by cropping and tillage systems. *J. Prod. Agric.* **1996**, *9*, 180–186. [[CrossRef](#)]
24. Van Staalduijn, M. Impact of grazing by large and small mammalian herbivores in a Mongolian forest steppe. In *The Impact of Herbivores in Mongolian Forest Steppe*; Plant Ecology Group, Department of Biology, Utrecht University: Utrecht, The Netherlands, 2005; Chapter 3; pp. 49–64.
25. Van Genuchten, M. A closed-form equation for predicting the hydraulic conductivity of unsaturated soils. *Soil Sci. Soc. Am. J.* **1980**, *44*, 892–898. [[CrossRef](#)]
26. Yanagawa, A.; Fujimaki, H.; Jamsran, U.; Okuro, T.; Takeuchi, K. Changes in Dominant perennial species affect soil hydraulic properties after crop abandonment in a semiarid grassland in Mongolia. *Eurasian Soil Sci.* **2019**, *52*, 1378–1390. [[CrossRef](#)]
27. Miyazaki, S.; Yasunari, T.; Miyamoto, T.; Kaihotsu, I.; Davaa, G.; Oyunbaatar, D.; Natsagdorj, L.; Oki, T. Agrometeorological conditions of grassland vegetation in central Mongolia and their impact for leaf area growth. *J. Geophys. Res. Atmos.* **2004**, *109*, 14. [[CrossRef](#)]
28. Miyasaka, K.; Shiozawa, S.; Nishida, K.; Siilegmaa, B.; Yoshida, S.; Undarmaa, J. Occurrence of water ponding on soil surfaces depending on infiltration rates on Mongolian rangeland. *Hydrol. Process.* **2017**, *31*, 3996–4005. [[CrossRef](#)]
29. Fan, J.; McConkey, B.; Wang, H.; Janzen, H. Root distribution by depth for temperate agricultural crops. *Field Crops Res.* **2016**, *189*, 68–74. [[CrossRef](#)]
30. Gan, Y.; Campbell, C.A.; Janzen, H.H.; Lemke, R.; Liu, L.; Basnyat, P.; McDonald, C.L. Root mass for oilseed and pulse crops: Growth and distribution in the soil profile. *Can. J. Plant Sci.* **2009**, *89*, 883–893. [[CrossRef](#)]
31. Cutforth, H.; Angadi, S.; McConkey, B.; Miller, P.; Ulrich, D.; Gulden, R.; Volkmar, K.; Entz, M.; Brandt, S. Comparing rooting characteristics and soil water withdrawal patterns of wheat with alternative oilseed and pulse crops grown in the semiarid Canadian prairie. *Can. J. Soil Sci.* **2013**, *93*, 147–160. [[CrossRef](#)]
32. Satho, T.; Sugita, M.; Yamanaka, T.; Tsujimura, M.; Ishii, R. Water dynamics within soil-vegetation-atmosphere system in a steppe region covered by shrubs and herbaceous plants. In *The Mongolian Network: Environmental Issues under Climate and Social Changes*; Ecological Research Monographs; Yamanaka, N., Fujita, N., Maekawa, A., Eds.; Springer: Tokyo, Japan, 2013; pp. 43–63.
33. Onda, Y.; Kato, H.; Tanaka, Y.; Tsujimura, M.; Davaa, G.; Oyunbaatar, D. Analysis of runoff generation and soil erosion processes by using environmental radionuclides in semiarid areas of Mongolia. *J. Hydrol.* **2007**, *333*, 124–132. [[CrossRef](#)]
34. Boyer, J.S. Leaf enlargement and metabolic rates in corn, soybean, and sunflower at various leaf water potentials. *Plant Physiol.* **1970**, *46*, 233–235. [[CrossRef](#)]
35. Turner, N.C. Drought Resistance: A Comparison of Two Research Frameworks. In *Management of Agricultural Drought: Agronomic and Genetic Options*; Saxena, N., Ed.; Science Publishers, Inc.: Enfield, NH, USA, 2003; pp. 89–102.
36. Jones, H.G. *Plants and Microclimate: A Quantitative Approach to Environmental Plant Physiology*; Cambridge University Press: Cambridge, UK, 2013.
37. Merrill, S.D.; Tanaka, D.L.; Hanson, J.D. Root length growth of eight crop species in haplustoll soils. *Soil Sci. Soc. Am. J.* **2002**, *66*, 913–923. [[CrossRef](#)]
38. Gan, Y.; Campbell, C.A.; Liu, L.; Basnyat, P.; McDonald, C.L. Water use and distribution profile under pulse and oilseed crops in semiarid northern high latitude areas. *Agric. Water Manag.* **2009**, *96*, 337–348. [[CrossRef](#)]

39. Nielsen, D.C.; Unger, P.W.; Miller, P.R. Efficient water use in dryland cropping systems in the Great Plains. *Agron. J.* **2005**, *97*, 364–372. [[CrossRef](#)]
40. Price, J.S.; Hobson, R.N.; Neale, M.A.; Bruce, D.M. Seed losses in commercial harvesting of oilseed rape. *J. Agric. Eng. Res.* **1996**, *65*, 183–191. [[CrossRef](#)]
41. Simard, M.J.; Legere, A.; Pageau, D.; Lajeunesse, J.; Warwick, S. The frequency and persistence of volunteer canola (*Brassica napus*) in Quebec cropping systems. *Weed Technol.* **2002**, *16*, 433–439. [[CrossRef](#)]
42. Pari, L.; Assirelli, A.; Suardi, A.; Civitarese, V.; Del Giudice, A.; Santangelo, E. Seed losses during the harvesting of oilseed rape (*Brassica napus* L.) at on-farm scale. *J. Agric. Engin.* **2013**, *44*, 633–636. [[CrossRef](#)]